

Effect of support structure on the activity of Cr/nanosilica catalysts and the morphology of prepared polyethylene

Zahra Mohamadnia,^a Ebrahim Ahmadi,^{b*} Mehdi Nekoomanesh,^{a*} Ali Ramazani^b and Hamid Salehi Mobarakeh^c

Abstract

Phillips-type catalysts are responsible for the commercial production of more than one-third of all polyethylene sold worldwide. Many types of chromium-based catalysts are used in the Phillips polymerization process. Ordered mesoporous silica structures were synthesized using various surfactant species. Chromium nitrate nonahydrate ($\text{Cr}(\text{NO}_3)_3 \cdot 9\text{H}_2\text{O}$) complex was grafted onto the surface of pure silica and was used for ethylene polymerization. The materials were characterized using X-ray diffraction, nitrogen adsorption-desorption, inductively coupled plasma optical emission spectroscopy, thermogravimetric analysis and Fourier transform infrared spectroscopy. In the as-synthesized materials, Cr^{3+} is present as a surface species in pseudo-octahedral coordination. After calcination, Cr^{3+} is almost completely oxidized to Cr^{6+} , which is anchored onto the surface in various oxidative states. The catalyst polymerization activity is dependent on the chromium loading, the pre-calcination temperature and the support properties. In particular, the chromium catalyst prepared using spherical SBA-15 is more active than the other catalysts investigated. Porous and nano-fibrous polyethylene samples were prepared using various silica-supported chromium catalytic systems. Differential scanning calorimetry results show that the melting point of samples produced with the SBA-15-supported catalyst is higher than that of samples produced with Cr/SiO_2 under the same conditions, which could be related to the existence of an extended-chain structure.

© 2010 Society of Chemical Industry

Keywords: mesoporous; ethylene polymerization; chromium catalyst; SBA-15

INTRODUCTION

In the early 1950s Hogan and Banks¹ discovered that chromium oxide supported on silica and other carriers would polymerize olefins to high polymers. Since then, this catalytic system has shown important developments, and nowadays Phillips-type catalysts are responsible for the commercial production of more than one-third of all polyethylene sold worldwide.² Many types of chromium-based catalysts are used in the Phillips polymerization process. The reason for this catalyst variety comes from the wide variations in the properties of the polymer depending upon its molecular structure.³

The activity of these polymerization catalysts is very sensitive towards (i) the chromium anchorage and subsequent activation and (ii) the textural properties of the support, particularly its porosity, both playing an important role in the resulting properties of the polyethylene produced.⁴ In 1992, the Mobil Oil research group presented a new family of materials, designated M41S. These materials are characterized by narrow pore size distributions, tunable from 15 to 100 Å, and large surface areas. The M41S class fills the gap between mesoporous materials obtained from pillaring of layered silicates and mesoporous gels and glasses. MCM-41 is the most predominant example of the M41S family and can be envisaged as a hexagonal tubular material with a very high surface area and sharply defined pore diameters in the range 2–10 nm.⁵

Ethylene polymerization over chromium supported on conventional MCM-41 has been previously reported,⁶ but activity values were lower than those obtained using conventional Cr/SiO_2 catalysts.

Studies based on chromium supported on these materials indicated that different chromium species can be anchored to the support surface depending on its nature. For example, Weckhuysen *et al.*⁷ found that monochromate is the dominant species in chromium supported on alumina, magnesium oxide and titanium dioxide; however, dichromate species predominate in chromium supported on silica. Pullukat *et al.*⁸ reported that the polymerization activity of chromium supported on alumina was one order of magnitude lower than that of chromium supported

* Correspondence to: Ebrahim Ahmadi, Chemistry Department, Zanjan University, PO Box 45195-313, Zanjan, Iran. E-mail: ahmadi@znu.ac.ir

Mehdi Nekoomanesh, Department of Polymerization Engineering, Iran Polymer and Petrochemical Institute (IPPI), PO Box 14965-115, Tehran, Iran. E-mail: m.nekoomanesh@ippi.ac.ir

a Department of Polymerization Engineering, Iran Polymer and Petrochemical Institute (IPPI), PO Box 14965-115, Tehran, Iran

b Chemistry Department, Zanjan University, PO Box 45195-313, Zanjan, Iran

c Department of Science, Iran Polymer and Petrochemical Institute (IPPI), PO Box 14965-115, Tehran, Iran

on silica. Furthermore, alumina-supported chromium catalysts produced polyethylene with higher molecular weight.^{8,9} The textural properties of the support also have a significant influence on the behaviour of Phillips catalysts. So, chromium supported on high pore volume silica presents a higher catalytic activity and therefore produces a lower molecular weight polyethylene with higher melt index. On the contrary, small pore size silica gives less active catalysts leading to high molecular weight polyethylene.^{4,10} Another example of the influence of the textural properties of the support was given by Spoto *et al.*¹¹ and Zecchina *et al.*¹² They observed that on Cr²⁺ silicalite, the spatial limitations imposed by the porous character of the solid depress the growth of the polymeric chains formed inside the zeolite channels, these chains being short and having spectroscopic features different from those of the longer chains formed on the external surface.

SBA-15 (see the Experimental section) was synthesized by Zhao *et al.*^{13,14} using amphiphilic triblock copolymers to direct the organization of silica species under strong acidic conditions. MCM-41 and SBA-15 have regular, cylindrical, ordered hexagonal pores, with narrow pore size distribution and large surface area. Furthermore, the geometrical shape of the nano-channels can serve as polymerization reactors to affect the pattern of monomer insertion and to control polymer chain structure, polymer chain arrangement and polymer morphology.^{15,16}

Ma and co-workers¹⁷ synthesized mesoporous silica microspheres for use as packing material in HPLC columns to separate both small aromatic molecules and large biomolecules such as proteins. However, the way we used spherical silica as a support to prepare Phillips catalysts and carry out ethylene polymerization has not been reported yet.

Here, we report the synthesis and characterization of several silica supports and their behaviour in ethylene polymerization after chromium incorporation by grafting. The influences of the structure of MCM-41, spherical and commercial silica on the catalytic activities and the morphologies of the polyethylene produced were investigated and compared.

EXPERIMENTAL

Materials

All manipulations involving air- and/or water-sensitive compounds were performed under nitrogen atmosphere using standard Schlenk technology. Triethylaluminium (TEAL), cetyltrimethylammonium bromide (CTABr) and Pluronic 123 triblock (ethylene oxide (EO) and propylene oxide (PO)) copolymer (EO₂₀-PO₇₀-EO₂₀) were purchased from Aldrich. Tetraethylorthosilicate (TEOS) and ethanol were obtained from Merck. Polymerization-grade ethylene was purified using three columns of KOH, CuO and 5 Å molecular sieves. Hexane was refluxed over sodium with benzophenone as an indicator and distilled under nitrogen atmosphere before use.

Preparation of supports

SBA-15 was synthesized according to the procedure described by Zhao *et al.*¹⁴ using Pluronic 123 as template. In a typical preparation, 4.0 g of Pluronic 123 was dissolved in 30 g of water and 120 g of 2 mol L⁻¹ HCl solution with stirring at 35 °C. Then 8.50 g of TEOS was added into the solution with stirring at 35 °C for 20 h. The mixture was aged at 80 °C overnight under static conditions. The solid product was filtered off, washed and air-dried at room temperature. The template was removed from the as-prepared mesoporous material by Soxhlet extraction with ethanol for 96 h.

MCM-41 supports were synthesized according to the procedure described by Greco *et al.*¹⁸ using CTABr as surfactant agent. In a typical preparation, 2.5 g of CTABr was dissolved in 120 g of water and 9.5 g of 2.5 wt% ammonium solution was added. Then 10 g of TEOS was added into the solution with stirring at room temperature for 1 h. The solid product was recovered, washed and air-dried at room temperature overnight. The template was removed from the as-prepared mesoporous material by calcination at 550 °C for 6 h with a heating rate of 5 °C min⁻¹ under pure nitrogen.

Spherical SBA-15 (SBA-15(Sp)) supports were synthesized using TEOS as the silica source, Pluronic 123 as template, CTABr as co-surfactant and ethanol as co-solvent.¹⁷ Typically, 0.3 g of Pluronic 123 and 0.05 g of CTABr were dissolved in a solution formed by mixing 6 mL of 2 mol L⁻¹ HCl, 3 mL of water and 2.5 mL of ethanol. Then, 1 mL of TEOS was added to the aqueous solution at room temperature under magnetic stirring. The mixture was aged at 80 °C for 5 h under static conditions and was then allowed to age at 130 °C for 12 h. A white precipitate was recovered by filtration, dried at 90 °C for 24 h and calcined in air at 550 °C for 6 h to remove the template.

Preparation of silica-supported catalysts

The chromium grafting procedure started with Soxhlet-extracted silica materials previously outgassed under vacuum conditions overnight. Then, 2 g of the silica material was stirred with 30 mL of chromium nitrate nonahydrate solution in dried methanol for 3 h under reflux. A solid product was recovered and thoroughly washed with methanol. Finally, the grafted materials were calcined in air at 550 °C for 3 h with a heating rate of 2.0 °C min⁻¹. Inductively coupled plasma optical emission spectroscopy analysis was used to obtain the supported chromium content (0.19 wt%).

Preparation of polyethylene in slurry phase

Ethylene polymerization reactions were carried out in a 2 L stainless steel stirred autoclave engineers apparatus. Reaction conditions were 800 rpm, 90 °C, 31.5 bar (3.15 MPa) ethylene pressure. An amount of 0.5 mol of TEAL was used with *n*-hexane as solvent. After 1 h of reaction, the resulting polyethylene (PE) was recovered, filtered, washed with acetone and dried for 6 h at 70 °C. Polymerization activities (kg PE g⁻¹ Cr⁻¹ h⁻¹) were calculated for each run.

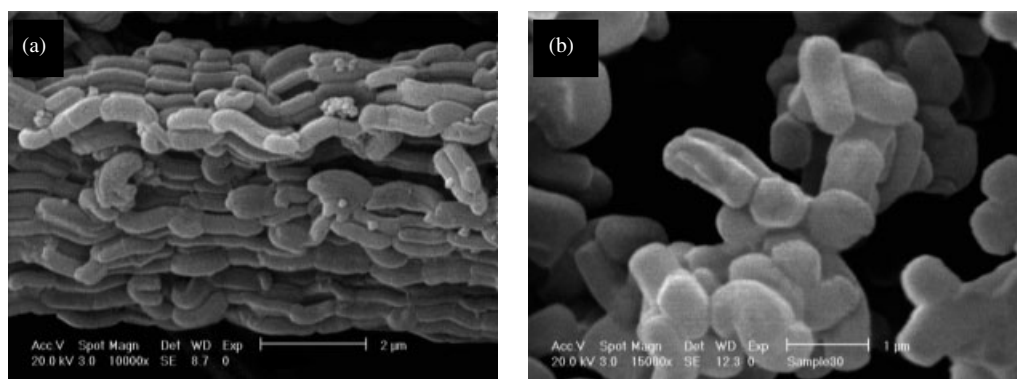
Characterization of support, chromium catalyst and PE

X-ray powder diffraction data were obtained with a D/max-3BX diffractometer using Cu K α radiation of wavelength 0.154 nm. Nitrogen adsorption-desorption isotherms were obtained at 77 K using an OMNISORPTM 100CX VER 1G adsorption apparatus. Samples were outgassed at 473 K for at least 8 h in vacuum prior to measurements. The supports and polymer samples were deposited on a sample holder and sputtered with gold. The morphologies were observed using a scanning electron microscope (SIRION, FEI, USA). DSC was carried out with a PerkinElmer DSC 7 instrument. Ultrahigh-purity nitrogen was purged through the calorimeter. The PE samples (*ca* 4 mg) were heated to 170 °C at a rate of 10 °C min⁻¹, and then they were cooled to 40 °C at a rate of 10 °C min⁻¹. Subsequently, a second heating cycle was conducted at a heating rate of 10 °C min⁻¹.

Table 1. Structural parameters^a of synthetic and commercial supports

Sample	Support	S_{BET} ($\text{m}^2 \text{g}^{-1}$)	d_p (Å)	V_p (mL g^{-1})	d_{100} (Å)	b_p (Å)
1	SiO ₂	500	60	0.75	74	12.7
2	SBA-15(Hex)	479	35.8	0.51	87	32.4
3	MCM-41	583.6	12.9	0.28	41	17.2
4	SBA-15(Sp)	894.5	106	3.6	103	6.5

^a S_{BET} , BET specific surface area; V_p , specific pore volume; d_p , average pore diameter, obtained from BJH adsorption data ($d_p = 4V_p/S_{\text{BET}}$); d_{100} , XRD interplanar spacing; b_p , pore wall thickness ($b_p = (a_0 - d_p)/2$; $a_0 = (2/\sqrt{3})d_{100}$).

**Figure 1.** SEM micrographs of SBA-15: (a) tubular structure of Soxhlet-extracted SBA-15; (b) calcined SBA-15.

RESULTS AND DISCUSSION

Characterization of SBA-15

The XRD pattern of as-synthesized SBA-15 prepared using Pluronic P123 shows four well-resolved peaks that can be indexed as (100), (110), (200) and (210) diffraction peaks associated with $p6mm$ hexagonal symmetry. Three additional peaks appear in the range of $2\theta = 2.5\text{--}3.5^\circ$ that can be indexed as (300), (220) and (310) scattering reflections. The intense (100) peak is associated with a d spacing of 87 Å, corresponding to a large unit cell parameter ($a = 90$ Å).^{13,14}

Table 1 summarizes the textural properties of the SBA-15 support derived from nitrogen adsorption–desorption isotherms and pore size distributions. Table 1 also gives the textural properties of commercial silica used as a reference support to prepare Cr/SiO₂ catalysts, for comparison purposes.^{13,14}

SEM was used to determine the size and morphology of SBA-15. The micrographs in Fig. 1 show that the SBA-15 particles have tubular structure with lengths of 0.9–1.5 μm and diameters of 0.2–0.3 μm. Each particle consists of many hexagonal nano-channels.

Characterization of MCM-41

The XRD pattern of MCM-41 shows four Bragg peaks: 100, 110, 200 and 210. The Bragg peaks show that MCM-41 has a quite uniform long-range ordered hexagonal symmetry.¹⁹ The textural properties of the MCM-41 support are summarized in Table 1.

The SEM micrographs in Fig. 2 show that the MCM-41 particles have tubular structure with lengths of 1–2 μm and diameters of 0.5–1 μm.

Characterization of SBA-15(Sp)

The particle morphology was microscopically examined using SEM (Fig. 3). As shown in Fig. 3(a), the sample obtained at 80 °C

for 5 h (SBA-15(Sp)₀) exhibits a perfectly spherical morphology with diameters ranging from 3 to 6 μm (Table 1). To examine the effect of ethanol on the morphology of the product, a synthesis was performed in the absence of ethanol with other reaction conditions kept similar to that for SBA-15(Sp)₀. The resulting product exhibits a mixture of many irregular particles and some microspheres (Fig. 3(b)).

The addition of co-solvent in the starting solution causes a decrease of the polarity of the solvent and thus a decrease the rate of nucleation and growth of the mesostructured products because of the slower TEOS hydrolysis and mesostructure assembly, which could contribute to the formation of silica spheres with smooth surfaces.^{20–22}

The small-angle X-ray diffraction pattern of SBA-15(Sp) (Fig. 4) shows Bragg peaks with d spacing of 10.3 nm which is attributed to ordered mesoporous materials with spherical structure.

Nitrogen adsorption–desorption isotherms and the corresponding Barrett–Joyner–Halenda (BJH) pore size distribution curves of SBA-15(Sp) are shown in Fig. 5. The material exhibits type IV isotherms with well-defined steps associated with the filling of the mesopores due to capillary condensation (Fig. 5(a)). The physicochemical properties of SBA-15(Sp) obtained are summarized in Table 1.

As shown in Fig. 5(b), the calculated average pore size for SBA-15(Sp) is 10.6 nm which is consistent with the XRD result. It is noted that the pore volume for SBA-15(Sp) is 3.6 cm³ g^{−1}, much higher than that for the hexagonal SBA-15 particles (0.51 cm³ g^{−1}; see Table 1). Preparation of hexagonal mesoporous silica using CTABr or Pluronic 123 templates with cationic silica materials in acidic condition was reported.²³

Preliminary results show that mesoporous silica products obtained in the presence of CTABr alone or Pluronic 123 alone under the current synthesis conditions do not exhibit spherical morphology, suggesting that the presence of both CTABr and

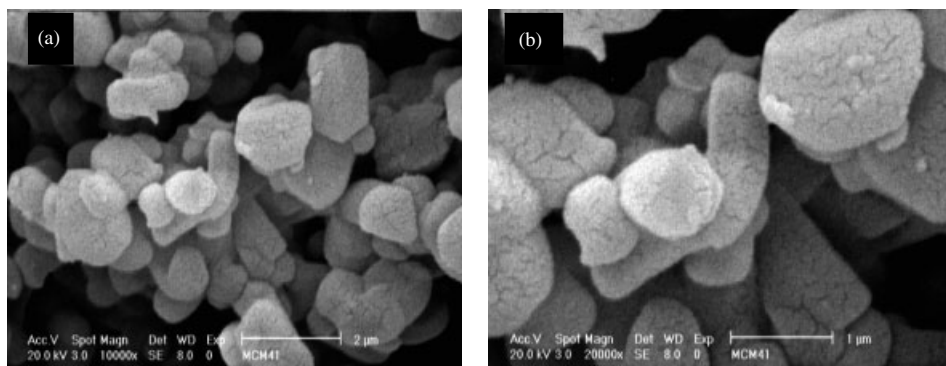


Figure 2. SEM micrographs of MCM-41: (a) hexagonal structure of MCM-41; (b) magnified view of (a).

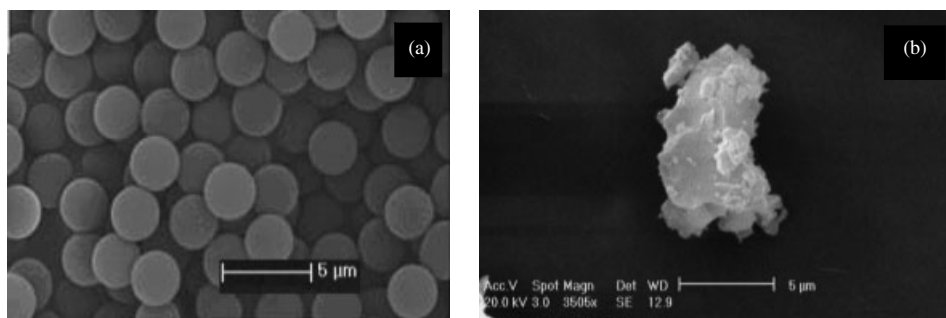


Figure 3. SEM micrographs of SBA-15(Sp) prepared at (a) 80 °C for 5 h, and (b) synthesized without ethanol co-solvent at 80 °C for 5 h followed with 130 °C for 12 h.

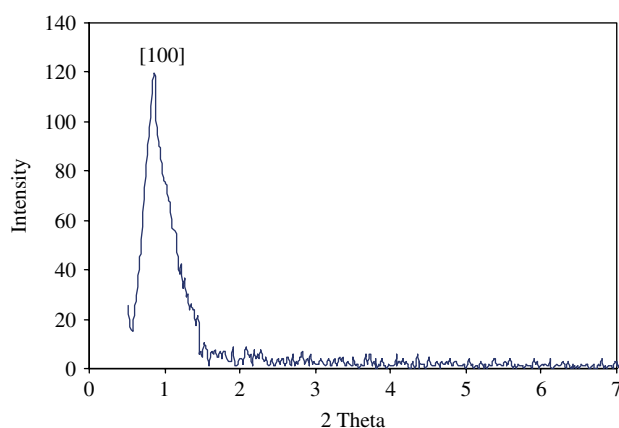


Figure 4. XRD pattern of spherical SBA-15(Sp).

Pluronic 123 is essential for the formation of the mesoporous silica spheres. In the present synthesis, the molar ratio between CTABr and Pluronic 123 is about 3 but the weight ratio between them is actually very low (1/6). Therefore, the Pluronic 123 polymer contributes largely to the final mesopores whereas the CTABr surfactant mainly plays a role of co-surfactant. The fact that the mesoporous silica obtained using the mixed Pluronic 123/CTABr templates shows a monodisperse rather than a bimodal pore size distribution indicates that the mesopores could be formed by the co-assembly of the mixed Pluronic 123/CTABr micelles with cationic silica species (Fig. 5(b)). Since the mixed Pluronic 123/CTABr micelles are not so uniform as the single Pluronic 123 or CTABr micelles, the final mesopore structure tends to lack a long-range hexagonal order.¹⁷

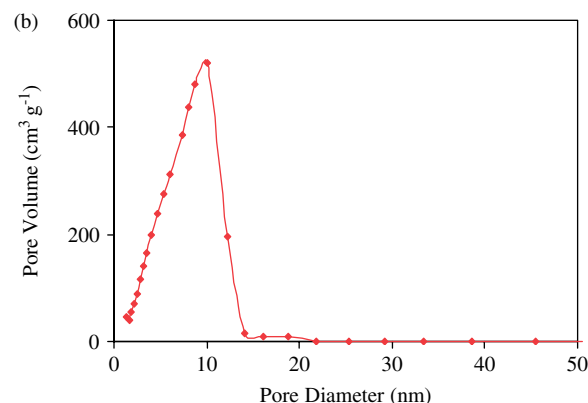
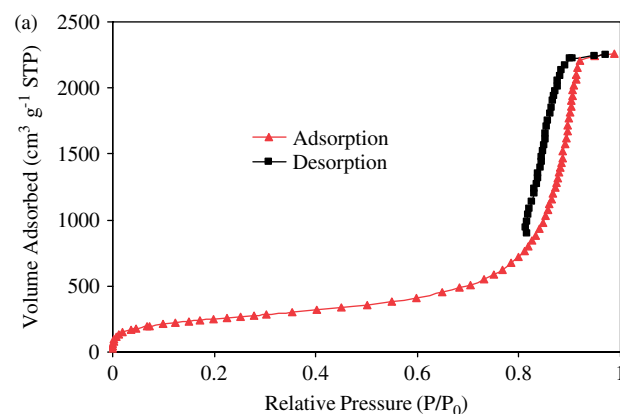


Figure 5. (a) Nitrogen adsorption–desorption isotherms and (b) pore size distribution curve from the adsorption branch of SBA-15(Sp).

Table 2. Results of ethylene polymerization with synthetic and commercial silica-supported chromium catalysts

Run ^a	Catalyst	Cr ⁻¹ h ⁻¹)	Activity (kg PE g ⁻¹ Density (g mL ⁻¹))	T_m^b (°C)		ΔH (J g ⁻¹)		Crystallinity ^c (%)
				First scan	Second scan	First scan	Second scan	
1	Cr/SiO ₂	13.4	0.21	138.9	135.2	170.4	150.4	58.0
2	Cr/SBA-15(Hex)	34	0.19	142.6	138.0	224.1	182.5	76.3
3	Cr/MCM-41	15	0.2	141.4	136.5	204.8	162.7	69.8
4	Cr/SBA-15(Sp)	175	0.26	141.6	135.9	198.7	164.4	67.7

^a Polyethylene pressure = 31.5 bar (3.15 MPa); solvent = hexane; co-catalyst = TEAL, T_p (polymerization temperature) = 90 °C.

^b Melting temperature measured using DSC analysis.

^c Crystallinity from XRD analysis.

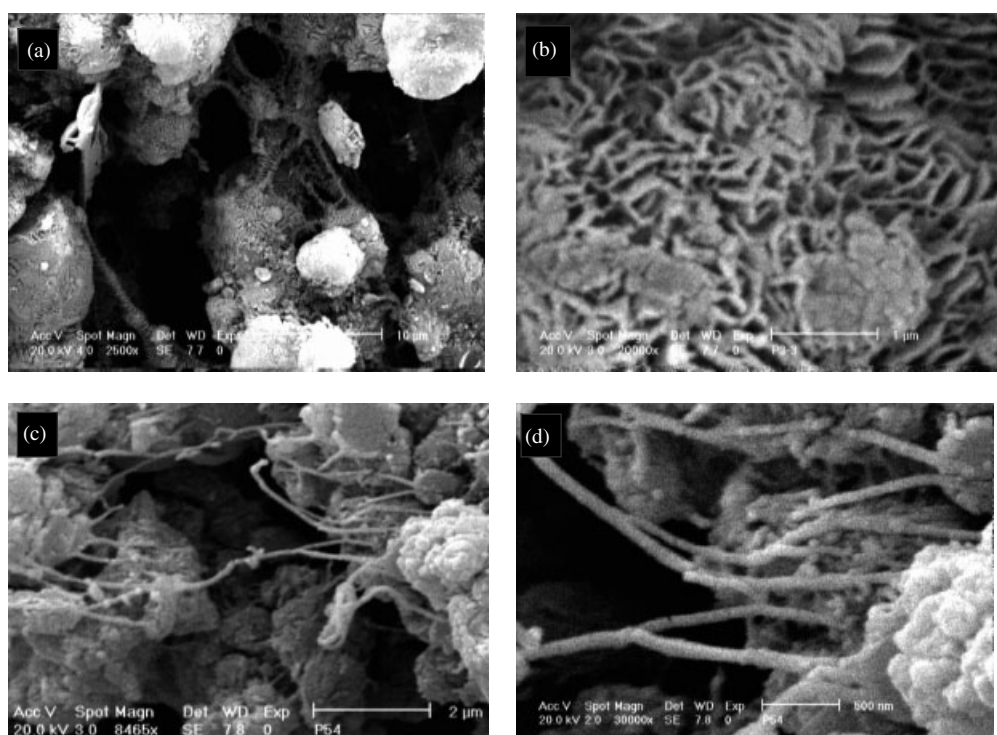


Figure 6. SEM micrographs of PE produced from supported chromium catalysts for polymerization at 90 °C: (a) Cr/SiO₂; (b) magnified view of (a); (c) Cr/SBA-15; (d) magnified view of (c).

Ethylene polymerization results

Chromium catalysts based on hexagonal SBA-15 (Cr/SBA-15)

The Cr/SBA-15 and Cr/SiO₂ catalysts were tested in ethylene polymerization. Table 2 gives the ethylene polymerization activities of the Cr/SBA-15 catalyst compared to the conventional Cr/SiO₂ catalyst prepared from commercial silica. Table 2 also gives the main properties of the resulting polymers: bulk density, melt temperature, enthalpy change and degree of crystallinity.

From the results of ΔH , the resulting PE has higher crystallinity compared to the PE prepared using the Cr/SiO₂ catalyst. The activity of Cr/SBA-15 is higher than that of Cr/SiO₂. Cr/SBA-15 catalyst prepared by impregnation gives PE with slightly higher melting temperature than the PE obtained from Cr/SiO₂ catalyst. This indicates that the channels of SBA-15 can control the direction of the chain propagation to increase the crystallinity of the PE.

A higher surface area might be expected to yield higher activity, which is often observed. However, the picture is more complicated

because the polymer immediately fills up the pores. If the catalyst structure is fragile enough it fragments into a very large number of smaller pieces which continue to produce polymer. If the structure is too rigid, fragmentation does not occur, the pores remain blocked by polymer and no subsequent activity is observed. Fragility is often correlated with pore volume.¹⁰

Figures 6(a) and (b) show SEM micrographs of the sample produced from run 1 of Table 2, which indicate the PE samples mainly take on porous morphologies. SEM micrographs of the sample produced from run 2 of Table 2 (Figs. 6(c) and (d)) mainly show a smooth nano-fibre morphology. The ethylene can disperse into the channels easily and polymerize in the channels that control the direction of the chain propagation to form fibres.

The SEM micrographs show that fibres and floccules are the major morphological units in the resultant samples. The diameter of the single nano-fibres is 50–300 nm. With an extension of polymerization time, the number of floccules increases.

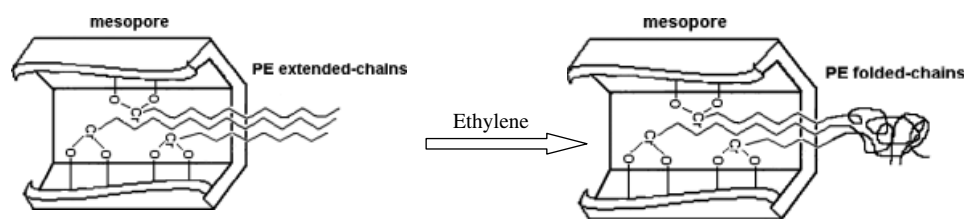


Figure 7. Possible formation process of floccules at low polymerization rate.

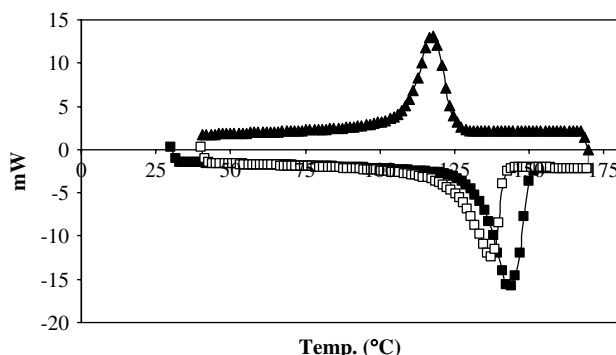


Figure 8. DSC thermograms of polyethylene produced by Cr/SBA-15 (a)(◇) Run1 (40–170 °C) 20 °C/min under pure N₂, (▲) Run2 (170–40 °C) –20 °C/min under pure N₂ and (■) Run3 (40–170 °C) 20 °C/min under pure N₂.

PE nano-fibres result from the control of SBA-15 nano-channels over the direction and dimension of PE chain propagation. The SBA-15 consists of a honeycomb-shaped array of unidimensional hexagonal pores²⁴ with the pore diameter (35.8 Å) being much smaller than the lamellar thickness (300 Å) of the folded-chain crystals of ordinary PE.²⁵ These nano-channels can serve as templates to suppress the kinetically favoured chain folding process, thus leading to PE extended chains. Then these extended chains growing out of the SBA-15 nano-channels aggregate and crystallize to form nano-fibres.²⁶ The nano-fibres then aggregate further to form fibre aggregates and bundles that are about 1 µm in size.

The appearance of PE floccules results from the changing polymerization rate. At the beginning of polymerization, the ethylene polymerizes at a rapid rate. Many extended chains grow out of SBA-15 channels simultaneously and aggregate easily to form fibres. With the extension of the polymerization time, the polymerization rate decreases, the extended chains

produced simultaneously are not enough to aggregate and then the extended chains may change into other folded chains again. Thus, with an extension of polymerization time, the amount of floccules increases. The possible process of formation of the floccules is shown in Fig. 7. From the results discussed above, it is evident that the proportion of nano-fibres and floccules in the PE samples can be controlled by changing the polymerization time.

DSC analysis was used for the thermal characterization of the PE produced from Cr/SBA-15(Hex) (Fig. 8). The DSC curve of polymer shows an exothermic peak at 142.6 °C ($\Delta H = 224.1 \text{ J g}^{-1}$) in comparison with melt-crystallized high-density polyethylenes (HDPEs; 133–135 °C), which indicates the presence of extended-chain crystals.²⁷ Once melted and recrystallized, the PE samples have significantly lower T_m and melting enthalpy (ΔH_m) values because of the formation of the folded-chain lamellar crystal structure.²⁸

As is evident from the second scan, recrystallization significantly decreases the melting point which may be related to degradation of PE nano-fibre (Fig. 9(b)). Crystallinity is 76.3% for nano-fibre samples.

The higher melting point may be related to a high molecular weight, long chains having a small number of side branches and nano-fibre formation. The gel permeation chromatography curve of polymers obtained from Cr/SBA-15 catalyst is shown in Fig. 10. It is obvious that the Cr/SBA-15 catalyst system produces PE with bimodal molecular weight distribution and high molecular weight. It is likely that the bimodal molecular weight distribution is due to PE formation from the chromium sites on the internal and external surfaces.

Figure 11 shows the XRD patterns of the PE prepared using the silica-supported catalysts. The typical [110] and [200] diffraction peaks at 21.4° and 23.8° testify to the orthorhombic crystalline structure. There is also a small amorphous halo around 19.50°, indicating the existence of floccules. With an increase in polymerization time, the intensity of the amorphous halo increases.²⁹ The results show that PE prepared from Cr/SBA-15(Hex) catalyst has the highest crystallinity among the PEs studied.

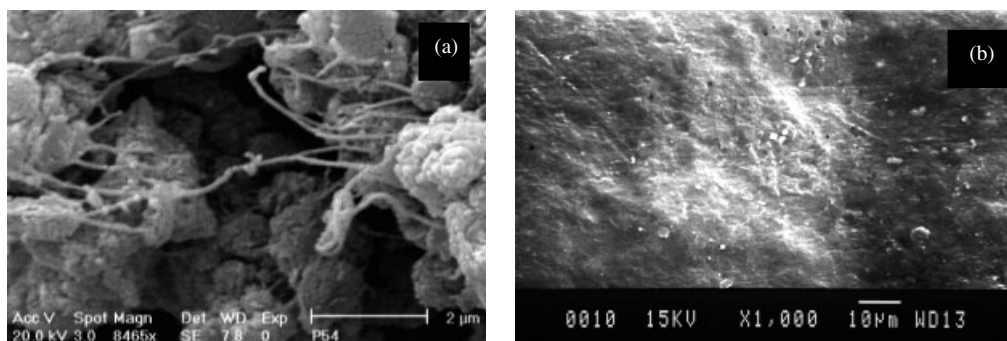


Figure 9. SEM micrographs of PE produced from Cr/SBA-15(Hex): (a) as-synthesized; (b) after recrystallization.

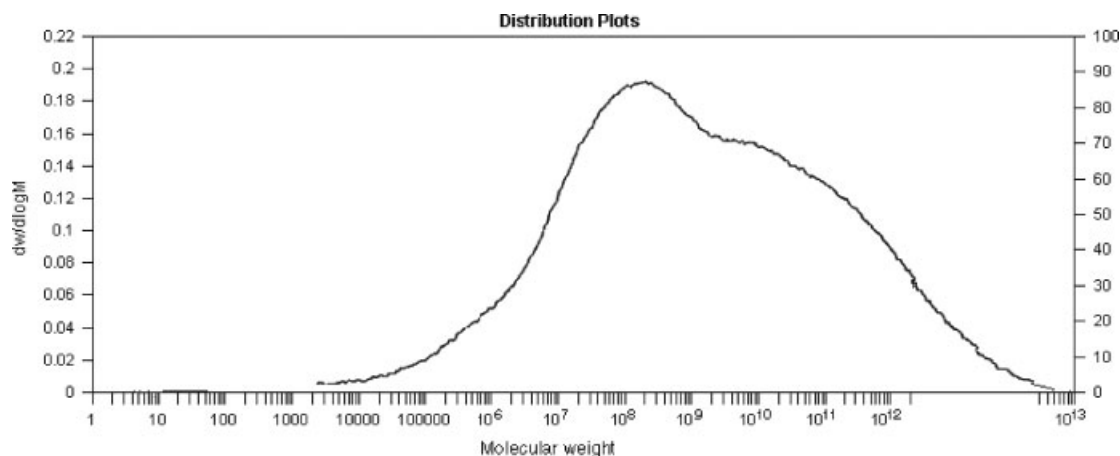


Figure 10. Gel permeation chromatography curve of polymer nano-fibre obtained using Cr/SBA-15.

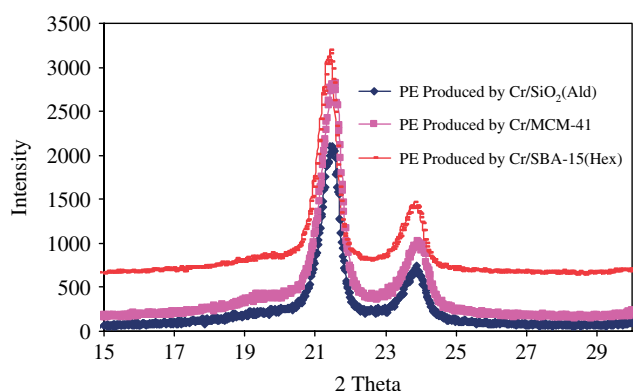


Figure 11. XRD spectra of PE samples prepared using silica-supported catalysts.

Chromium catalysts based on MCM-41 (Cr/MCM-41)

Table 2 gives the polymerization results for Cr/MCM-41 catalyst. The activity of Cr/MCM-41 is $15 \text{ kg PE g}^{-1} \text{ Cr}^{-1} \text{ h}^{-1}$ which is similar to that of Cr/SiO₂ catalyst. The melting point of the PE prepared using Cr/MCM-41 catalyst is higher than that of the PE prepared using Cr/SiO₂ catalyst (Fig. 12). In Fig. 12 the high melting point of the polymers prepared using Cr/MCM-41 and Cr/SiO₂ in comparison with that of HDPE may be attributed to the high molecular weight, long chains having a small number of side branches and nano-fibre formation.^{27,28} As is evident from the second scan, recrystallization significantly decrease the melting point which may be related to degradation of PE nano-fibres. Crystallinity is 69.8% for nano-fibre samples.

Figure 13 shows the XRD spectra of the PE samples prepared with Cr/SiO₂ and Cr/MCM-41. The typical [110] and [200] diffraction peaks at 21.5° and 23.9° testify to the orthorhombic crystalline structure. There is also a small amorphous halo around 19.50°, indicating the existence of folded chains. With an increase in polymerization time, the intensity of the amorphous halo increases.²⁹ The results show that PE prepared using Cr/MCM-41 catalyst has higher crystallinity than that prepared using Cr/SiO₂.

According to Figs 14(a) and (b), the PE samples have nano-fibre morphologies with smooth surfaces. This indicates that the channels of MCM-41 can control the direction of the chain propagation to increase the crystallinity of the PE and nano-fibre formation.

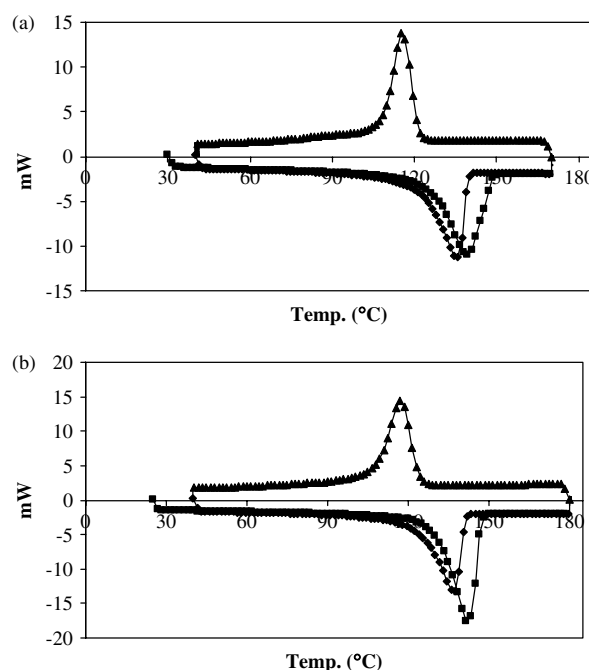


Figure 12. DSC thermogram of polyethylene produced by (a) Cr/SiO₂(Ald) 15 and (b) Cr/MCM-41 catalysts. (◇) Run1 (40–170 °C) 20 °C/min under pure N₂, (▲) Run2 (170–40 °C) –20 °C/min under pure N₂ and (■) Run3 (40–170 °C) 20 °C/min under pure N₂.

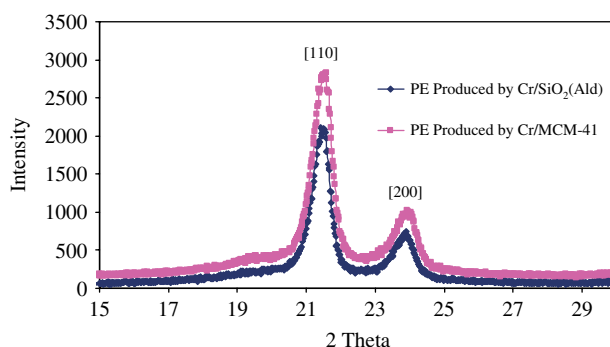


Figure 13. XRD spectra of PE samples prepared using silica-supported catalysts.

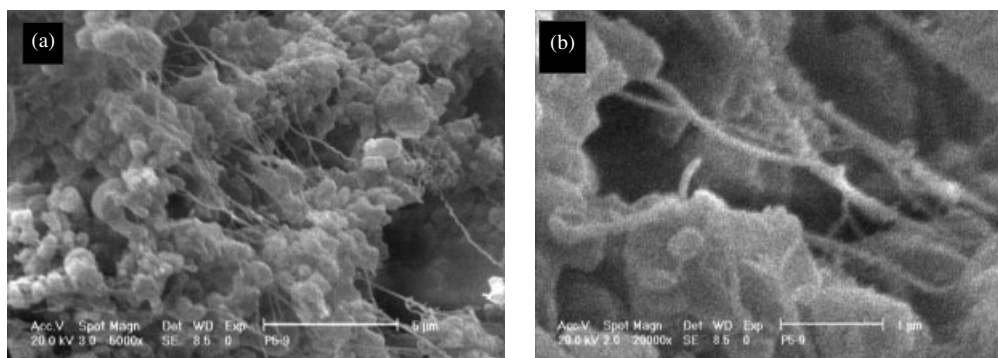


Figure 14. SEM micrographs of PE produced from supported chromium catalyst for polymerization at 90 °C: (a) Cr/MCM-41; (b) magnified view of (a).

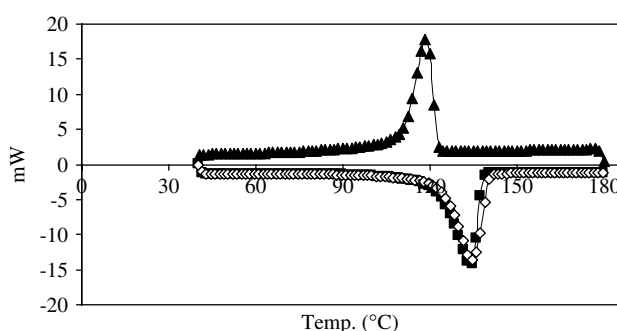


Figure 15. DSC thermograms of polyethylene produced by Cr/SBA-15(Sp) catalysts. (◇) Run1 (40–170 °C) 20 °C/min under pure N₂, (▲) Run2 (170–40 °C) –20 °C/min under pure N₂ and (■) Run3 (40–170 °C) 20 °C/min under pure N₂.

Figure 14(a) shows the micro-fibres with the PE floccules at the end of the fibres and Fig. 14(b) shows single nano-fibres. The SEM micrographs show that the fibre morphology is the major one in the PE samples; the diameter of a single nano-fibre is 50–100 nm. With an extension of polymerization time, the numbers of floccules increase. Also there is some porous PE among the fibre floccules. A comparison between Figs 6 and 14 shows that the nano-fibres prepared using SBA-15-supported catalyst are larger in diameter than those prepared using MCM-41-supported catalyst. This result is due to the difference in the pore diameter between SBA-15 and MCM-41. SBA-15 has larger pore diameter than MCM-41, containing more PE chains in the pore.

Chromium catalysts based on spherical SBA-15 (Cr/SBA-15(Sp))

Table 2 gives the polymerization results for Cr/SBA-15(Sp) catalyst. The activity of Cr/SBA-15(Sp) is 175 kg PE g^{−1} Cr^{−1} h^{−1} which is higher than that of the previously discussed catalysts. This result is related to the high specific surface area (894.5 m² g^{−1}) and high pore volume (3.6 mL g^{−1}) of SBA-15(Sp) compared to the other supports (Table 1). Small pore size and pore volume, high pore diameter and internal chromium are responsible for the low polymerization activity of Cr/SBA-15 catalyst compared to Cr/SBA-15(Sp) catalyst. Active internal chromium sites would be quickly blocked with the polymer and the activity will decrease.³⁰

So increasing the pore size and pore volume leads to a higher activity of Phillips catalysts.³¹ The high pore volume and pore size, and small wall thickness of SBA-15(Sp) are responsible for high activity and the brittleness of the polymer. The polymerization activity of Cr/SBA-15(Sp) catalyst is significantly

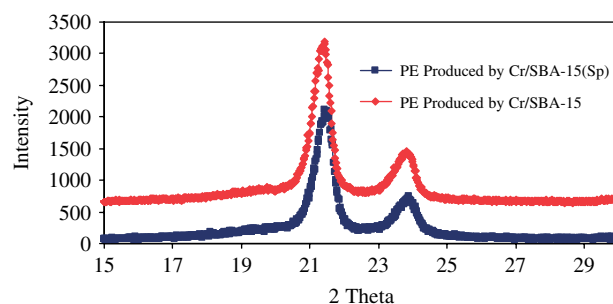


Figure 16. XRD spectra of PE samples prepared using silica-supported catalysts.

improved by the absence of nano-channels in the support; in hexagonal SBA-15, the presence of nano-channels blocks the active chromium sites and decreases the polymerization activity.

The DSC curve of the polymer shows an exothermic peak at 141.6 °C ($\Delta H_m = 198.7 \text{ J g}^{-1}$) which may be attributed to a melting point (Fig. 15) that is similar to the PE discussed above. As is evident from Table 2, this polymer shows a higher melting point than HDPE ($T_m = 133\text{--}135^\circ\text{C}$).

Figure 16 shows the XRD spectra of the samples prepared with Cr/SBA-15(Sp) and Cr/SBA-15. The typical [110] and [200] diffraction peaks at 21.5° and 23.9° testify to the orthorhombic crystalline structure. There is also a small amorphous halo around 19.50°, indicating the existence of amorphous PE.²⁹ A shift in the diffraction peaks towards higher 2 θ shows that the lamellar thickness of PE prepared from Cr/SBA-15(Sp) is less than that of the PE prepared from Cr/SBA-15. The results show that the PE prepared from Cr/MCM-41 catalyst has higher crystallinity than that from Cr/SiO₂. Different degrees of crystallinity may be attributed to different structures of silica-supported catalysts which is consistent with the DSC results given in Table 2. The channels of MCM-41 can control the direction of the chain propagation to increase the crystallinity of the PE.

According to Figs 17(a) and (b), SEM micrographs of the sample produced from run 4 of Table 2 show that the PE samples mainly take on porous morphologies.

As shown in Fig. 18, the amount of fine and coagulated polymer produced from Cr/SBA-15(Sp) is 67 and 30%, respectively. The particle size distribution of the polymer is between 250 and 500 μm and approximately uniform.

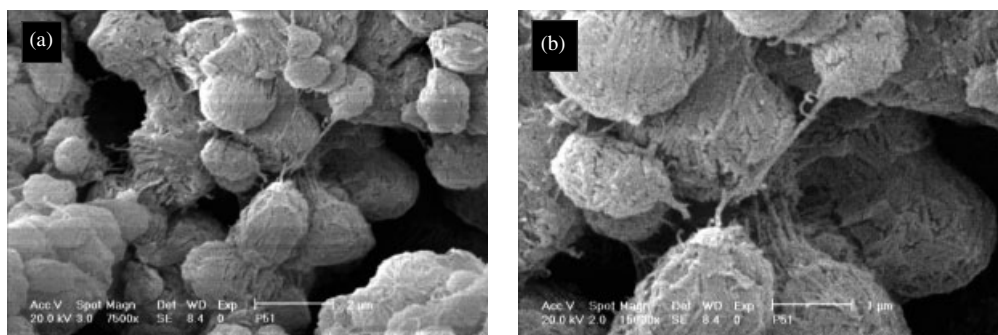


Figure 17. SEM micrographs of PE produced from supported chromium catalysts for polymerization at 90 °C: (a) Cr/SBA-15(Sp); (b) magnified view of (a).

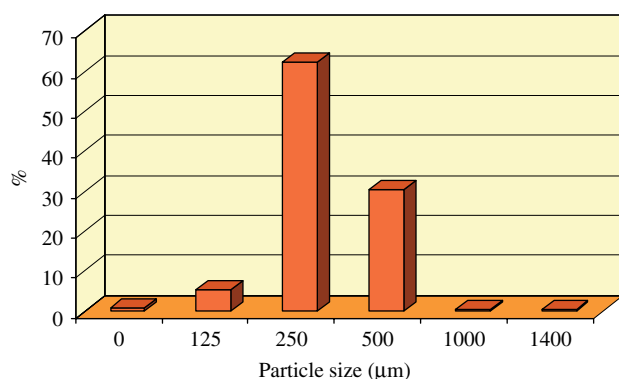


Figure 18. Particle size distribution of PE prepared from Cr/SBA-15(Sp) catalyst.

CONCLUSIONS

Nano-fibrous and porous PE were prepared via *in situ* ethylene polymerization, using SBA-15(Hex)- and SBA-15(Sp)-supported chromium catalytic systems. The melting point of the nano-fibrous PE was slightly higher than that of common PE. The diameters of the resultant fibres prepared with SBA-15-supported catalyst were larger than those prepared with MCM-41-supported catalyst.

Cr/SBA-15(Sp) catalyst showed the highest activity among the Cr/silica catalysts under investigation. According to the results, SBA-15(Sp) is a promising support to prepare new Phillips-type catalysts with high polymerization activity. The high pore volume and pore size, and small wall thickness of SBA-15(Sp) are responsible for the high polymerization activity and brittleness of the polymer formed using the Cr/SBA-15(Sp) catalyst. Polymers obtained with all the catalysts showed melting temperatures, bulk densities and load melt indexes commensurate with the formation of linear high-density PE.

ACKNOWLEDGEMENTS

The authors are grateful to Petrochemical Research and Technology Company and Iran Polymer and Petrochemical Institute for their financial support.

REFERENCES

- Hogan JP and Banks RL, Polymers and production thereof. US Patent 2825721 (1958).
- Weckhuysen BM and Schoonheydt RA, *Catal Today* **51**:215–221 (1999).
- McDaniel MP, *Ind Eng Chem Res* **27**:1559–1564 (1988).
- McDaniel MP, *Adv Catal* **33**:47–98 (1985).
- Weckhuysen BM, Ramachandra RR, Pelgrims J, Schoonheydt RA, Bodart P, Debras G, *et al*, *Chem Eur J* **6**:2960–2970 (2000).
- Rao RR, Weckhuysen BM and Schoonheydt RA, *Chem Commun* 445–446 (1999).
- Weckhuysen BM, Wachs IE and Schoonheydt RA, *Chem Rev* **96**:3327–3349 (1996).
- Pullukat TJ, Hoff RE and Shida MJ, *Polym Sci Polym Chem Ed* **18**:2857–2866 (1980).
- Conway SJ, Falconer JW and Rochester CH, *J Chem Soc Faraday Trans I* **85**:71–79 (1989).
- McDaniel MP, Uit DR and Benham EA, *J Catal* **176**:344–351 (1998).
- Spoto G, Bordiga S, Garrone E, Ghiotti G and Zecchina A, *J Mol Catal* **74**:175–184 (1992).
- Zecchina A, Spoto G, Ghiotti G and Garrone E, *J Mol Catal* **86**:423–446 (1994).
- Zhao D, Feng J, Huo Q, Melosh N, Fredrickson GH, Chmelka BF, *et al*, *Science* **279**:548–552 (1998).
- Zhao D, Huo Q, Feng J, Chmelka BF and Stucky GD, *J Am Chem Soc* **120**:6024–6036 (1998).
- Dong X, Wang L, Jiang G, Zhao Z, Sun T, Yu H, *et al*, *J Mol Catal A: Chem* **240**:239–244 (2005).
- Kresge CT, Leonowicz ME, Roth WJ, Vartuli JC and Beck JS, *Nature* **359**:710–712 (1992).
- Ma Y, Qi L, Ma J, Wu Y, Liu O and Cheng H, *Colloids Surf A: Physicochem Eng Aspects* **229**:1–8 (2003).
- Greco PP, Brambilla R, Einloft S, Stedile FC, Galland GB, dos Santos JHZ, *et al*, *J Mol Catal A: Chem* **240**:61–66 (2005).
- Grun M, Unger KK, Matsumoto A and Tsutsumi K, *Micropor Mesopor Mater* **27**:207–216 (1999).
- Kosuge K and Singh PS, *Chem Mater* **13**:2476–2482 (2001).
- Zhao D, Sun Q and Stucky GD, *Chem Mater* **12**:275–279 (2000).
- Zhao JW, Gao F, Fu YL, Jin W, Yang PY and Zhao DY, *Chem Commun* 752–753 (2002).
- Ying JY, Mehnert CP and Wong MS, *Angew Chem Int Ed* **38**:56–77 (1999).
- Beck JS, Vartuli JC, Roth WJ, Leonowicz ME, Kresge CT and Schmitt KD, *J Am Chem Soc* **114**:10834–10843 (1992).
- Tajima K and Aida T, *Chem Commun* 2399–2412 (2000).
- Kageyama K, Tamazawa JI and Aida T, *Science* **285**:2113–2115 (1999).
- Chanzy HD, Bonjour E and Marchessault RH, *Colloid Polym Sci* **252**:8–14 (1974).
- Ye Z, Zhu S, Wang WJ, Alsayouri H and Lin YS, *J Polym Sci B: Polym Phys* **41**:2433–2443 (2003).
- Krimm S and Toblosky AV, *J Polym Sci* **7**:57–76 (1951).
- Calleja G, Aguado J, Carrero A and Moreno J, *Catal Commun* **6**:153–157 (2005).
- Calleja G, Aguado J, Carrero A and Moreno J, *Appl Catal A: Gen* **316**:22–31 (2007).